APPENDIX G

Remote sensing methods to assess the effects of tree thinning on evapotranspiration rates in the Sacramento Mountains

This document describes work done by Peter ReVelle, Hydrology masters student, NMT, to assess the effects of tree thinning on evapotranspiration rates in the Sacramento Mountains.

New Mexico Bureau of Geology and Mineral Resources

A division of New Mexico Institute of Mining and Technology

Socorro, NM 87801
(575) 835 5490
Fax (575) 835 6333
www.geoinfo.nmt.edu

Remote sensing methods to assess the effects of tree thinning on evapotranspiration rates in the Sacramento Mountains

Peter ReVelle

Introduction

The largest component of the water budget and one of the most difficult to quantify accurately is the total water lost from the surface both as evaporation and by plants through leaves during transpiration [Newman et al., 2006]. Transpiration is a process in vegetation where water evaporates into the air through small openings in their leaves. The total water lost to the atmosphere as vapor is difficult to separate into evaporation and transpiration and is often lumped together and referred to as evapotranspiration (ET). In water-limited ecosystems in semi-arid and arid regions, ET can constitute 95% or more of the water budget [Newman et al., 2006]. Quantifying the amount of ET therefore is of critical importance in water-limited environments such as New Mexico for estimating the impact of thinning vegetation on the local water-balance and determining groundwater recharge. The response of the amount of ET in the experimental plots that were thinned in the Sacramento Mountains watershed were determined through analysis of satellite imagery.

Methods

Remote sensing is recognized as the only current viable method for mapping regional and larger meso-scale patterns of ET on Earth's surface [Kalma et al., 2008]. Remote sensing of ET provides a critical tool as a reliable means of obtaining low cost spatially distributed ET measurements where no comparable ground-based measurement technique is available [Karimi and Bastiaanssen, 2015]. Through applying remote sensing algorithms to satellite imagery, we calculate high resolution maps of ET for the Sacramento Mountains watershed area to improve estimates of ET before and after thinning. Images were obtained from the LANDSAT operational satellite. Currently it is the only satellite with the data necessary to perform remote sensing analysis at a spatial resolution needed to examine ET at the scale of the experimental plots in the watershed. The model used for remote sensing analysis, Mapping Evapotranspiration at High Resolution with Internal Calibration (METRIC), uses a physics based approach that calculates the energy balance spatially across an image to estimate ET for each pixel that represents an area 30 meters by 30 meters [Allen et al., 2007; Allen et al., 2011]. The latent heat flux (the amount of energy associated with evaporating a quantity of water) is calculated for each pixel from the energy balance:

$$\lambda E = R_n - G - H \quad (1)$$

In equation (1), λE represents the latent heat flux (W m^{-2}), R_n is the net radiation (W m^{-2}), G is the soil heat flux (W m^{-2}), and H is the sensible heat flux (W m^{-2}) which is the transfer of heat (or thermal energy) between the surface and the air. The ET is calculated by dividing by the latent heat of vaporization of water.

METRIC utilizes a custom calibration for each image where extreme conditions are determined and carefully selected as anchor pixels [Allen et al., 2007; Allen et al., 2011]. In the calibration METRIC uses weather data from ground instrumentation to adjust ET estimates based on ET calculated near agricultural fields using a standardized Penman-Montieth equation for a tall reference crop. Extreme conditions are chosen within agricultural fields and one pixel is selected for the hot, dry condition where the latent heat flux (λE) is set to 0 and the sensible heat flux (H) is set equal to the available energy ($R_n - G$). At the other pixel used for the wet, cold condition the latent heat flux is set to be equal to the available energy ($R_n - G$) and the sensible heat flux (H) is set equal to 0. The sensible heat transfer equation is inverted with the sensible heat flux (H) at each of the conditions used to determine the near-surface temperature difference at these points. The two points are then used to interpolate the near-surface temperature difference as a linear function of surface temperature which allows calculation of the sensible heat flux for each pixel based on its radiometric surface temperature.

In the mountains several improvements are made to the energy balance procedure used in METRIC through incorporating a Digital-Elevation-Model (DEM) at the same scale of the LANDSAT pixels. The geometry of the land surface for each pixel including the slope and orientation is taken into account for calculating the solar radiation reaching the surface at the given time of the day for a certain day of the year based on the varying sun angle with respect to each surface pixel [Allen et al., 2007]. Other improvements to METRIC have been made that incorporate the impacts of tall vegetation in sparse canopies where significant shading and scattering of solar radiation occurs with recent results showing improved estimates of ET of areas with both rain-fed and irrigated tall vegetation [Pôças, 2014]. The improvement to the methods used in METRIC as well as other refinements based on results from testing METRIC across different areas and settings were applied in the METRIC analysis of LANDSAT images within the Sacramento Mountains. Remote sensing analysis with METRIC enables quantifying 90 meter by 90 meter plot-scale ET before and after thinning.

Utilizing the ET maps produced using METRIC, differences in ET between thinned and control plots in the Sacramento Mountains watershed were evaluated before and after thinning. The net impact of thinning on ET for an image was quantified following a Before-After Control-Impact (BACI; Smith, 2002) approach commonly used in environmental impact assessment studies [Dore et al., 2012]. In the BACI method pre-thinning differences in ET between each pair of thinned and its associated control plots are subtracted from the post-thinning differences between that same pair at a given time of the year. Since continuous data is not available for satellite images, images were chosen that could be compared at nearly the same day of the year before and after thinning following the BACI method. Comparison at the same time of the year is used to control for or at least minimize the differences (due to soil moisture and precipitation) in the natural variability of ET in the area with time of the year not associated to thinning. Images were selected that had similar prior rainfall conditions with significant rain not occurring in the previous week in order to not overestimate the amount of ET representative for the associated time-period. Images from May 10, 2009 and May 13, 2010 were chosen for comparison based on early to mid-season growth representing an average period in the growing season somewhere between the expected peak mid to late season ET and the lower ET seen in early and very late season periods. In order to eliminate the effect of daily weather conditions on the before-after comparison we do not compare ET but ETrF values.

Results

Two LANDSAT images were analyzed using METRIC to calculate ET before and after thinning took place in fall of 2009. To enable better visual comparison and eliminate the effect of differences in daily weather, maps of ETrF (actual ET divided by a daily reference crop ET) were compared for May, 2009 and May, 2010. ETrF is a way of normalizing daily ET estimates based on a potential ET for a 0.5 meter tall reference crop which will vary with daily meteorological conditions and the amount of solar radiation. The ETrF maps are calculated by dividing METRIC's daily ET values calculated using an energy balance calculated for forest vegetation based on the Evaporative Fraction (EF) method commonly used for native vegetation. The METRIC ET was then divided by the tall reference crop daily ET to produce the final ETrF values. The results displayed in Figure 1 show very similar overall patterns for much of the watershed area between May images of both years but significant and variable decreases in the thinned plots in 2010 after thinning.

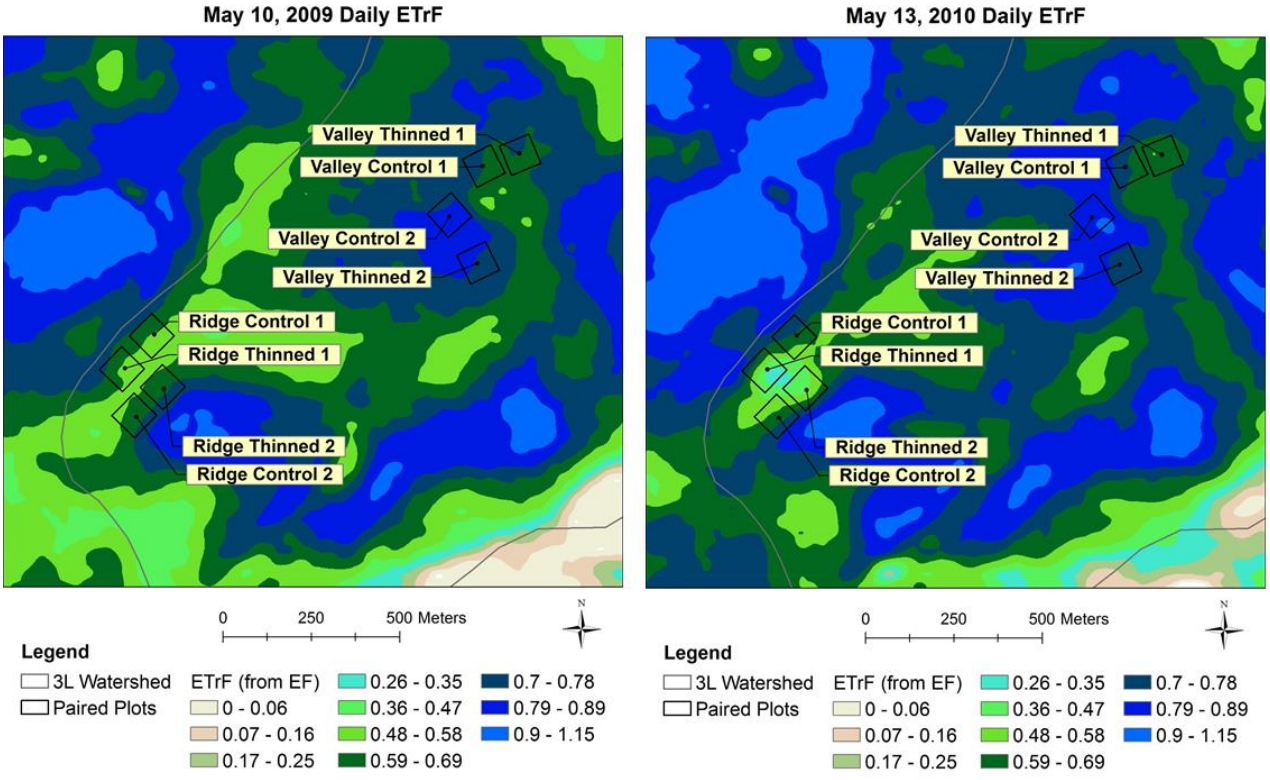

Figure 1. METRIC maps of daily ETrF from before (May 10, 2009) and after (May 13, 2010) from LANDSAT images.

An additional LANDSAT image in the 2009 season prior to treatment was analyzed with METRIC. To enable comparison between images, thinned plot ET values were subtracted from their associated control plot to compare their similarity as a percent difference. Figure 2 shows the percent difference in ET for the thinned plot relative to its control plot for May 10, 2009; July 29, 2009; and May 13, 2010.

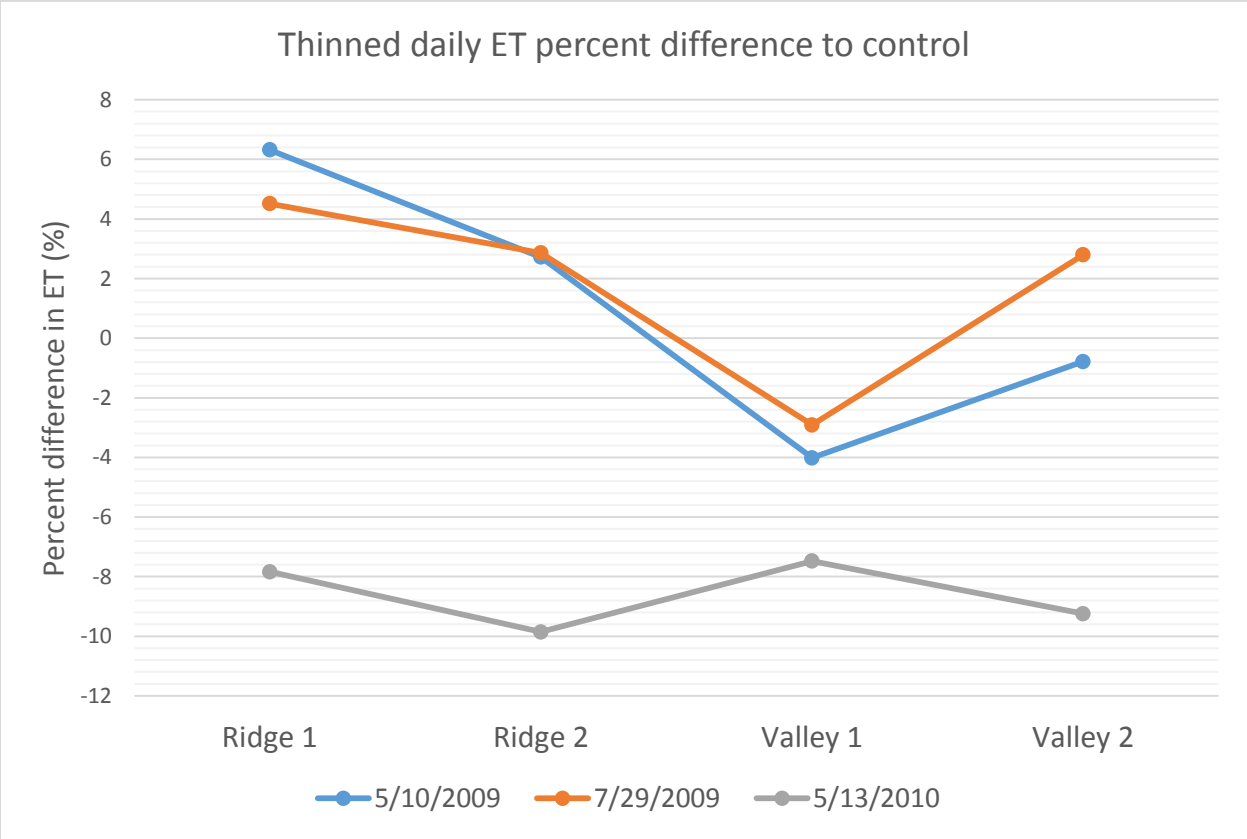

Figure 2. Comparison of thinned minus control percent difference for each set of plots for two days before thinning (May 10, 2009 and July 29, 2009) and May 13, 2010.

Pre-thinning differences in 2009 in May and July images show similar differences between each pair of thinned and control plots. Differences after treatment for May 13, 2010 shows significant deviations from the pre-thinning differences with significant decreases in the thinned ET relative to the control ET for each plot.

The statistical analysis of the differences in actual ET were compared following a Before-After Control-Impact (BACI) type analysis [Smith et al., 2002; Dore et al., 2013]. Since some of the control plots, especially in the valley, had relatively high differences in ET compared to their thinned plot prior to treatment, an additional control plot for each thinned pot was selected. Plots were chosen that matched the terrain and calculated pre-thinning characteristics of the thinned plots as well as or better than the original controls. These plots increased the number of data points and improved the estimates of the variability of ET within each area to improve the uncertainty in net ET differences after thinning. A two-sample t-test was performed on the difference between post-thinning and pre-thinning differences for each plot area and a 98% confidence interval was estimated for the net impact on ET for the thinned plots. The resulting

net impact on ET for each plot after thinning and associated confidence interval is shown in Figure 2.

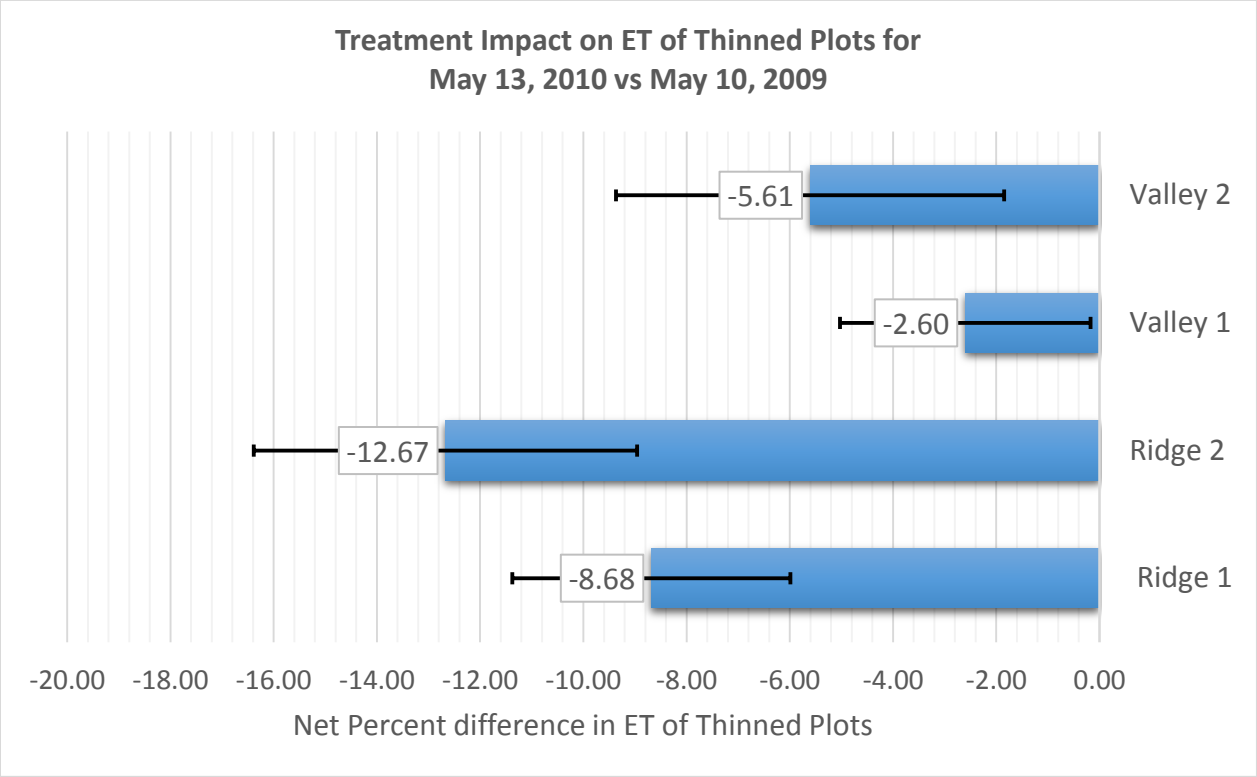

Figure 3. Comparison of net impact on daily ET of thinned plots determined from May, 2009 before thinning and May, 2010 after thinning images. Error bars represent the margin of error determined from a two-sample t-test at a significance level of 0.02. Larger percent reductions in forest density in the ridge plots than the valley plots correspond with the larger net decreases in ET.

Figure 2 shows that estimates of ET derived from METRIC indicate a significant net reduction in ET for all of the thinned plots but the magnitude of this net reduction in ET varies between different plots.

Discussion / Conclusions

The ETrF maps produced by METRIC show small-scale variability within the watershed that are difficult individually to compare to other estimates. As a whole, the values fall within estimates of ETrF values (usually referred to as the crop coefficient or K_c for agricultural crops) in the literature for mixed coniferous forests. Forest vegetation ETrF values in the literature show some variation between studies that were derived using different methods but generally range between 0.70 and 1 [McWhorter and Sunada, 1974; Verstraeten et al, 2005]. These values compare well with the average ETrF found for the May, 2009 and May, 2010 images for the overall watershed area around 0.65 to 0.70 and max values very close to 1.0 (1.01 – 1.02). In terms of the effect, the net impact on ET of ridge plots are within a few percent of the annual thinning effect found by Dore et al. [2012] in a similar upland semi-arid coniferous forest using ground-based ET measurements. In the first year after a 70% reduction in forest density Dore et al. [2012] found that the thinned area showed a net reduction in ET of -12%. The spatial scale of the thinned and control areas in Dore et al. [2012] were much larger than the thinned plots in this

study but compare well to the -8.7% and 12.7% reduction found in the ridge plots that were thinned by similar amounts.

Patterns in the net impact on ET appear to reflect the differences in treatment and the small differences in terrain within groups and the larger differences between different groups. Differences between the effects on ET for the ridge plots are likely due to the difference in aspects of the two ridge areas being along opposite sides of the same ridge and the difference this has on the daily solar radiation reaching these areas. Differences within groups between thinned and paired control plots are inevitability difficult to completely minimize in any natural system, especially for a highly non-linear process such as ET that is sensitive to variations in soil, vegetation, terrain and micrometeorology. However, similar ET differences prior to thinning within groups for different images around the same time of the season show relatively consistent and small variations in these differences that contrast with the large ET decreases found in the May 13, 2010 image shown in Figure 2. Using an additional control plot is believed to provide an improved estimate of the net impact and associated uncertainty on ET for each of the thinned plots. To evaluate the overall accuracy of these results and not just from the sampling variation shown in the data, the overall accuracy of METRIC and remote sensing ET estimates should also be considered.

Studies recently reviewed in Karimi and Bastiaanssen [2015] show consistently small errors in remotely sensed ET estimates in a variety of environmental settings and terrain. METRIC has shown some of the lowest errors of 1 to 2% in agricultural crop areas compared to ground-based ET estimates. Annually derived ET estimates reported in Karimi and Bastiaanssen [2015] show a range of mean absolute percent error from 1 to 20% with an average of 5.4% and a standard deviation of 5.0% [Karimi and Bastiaanssen 2015]. At the river-basin scale where water accounting can be done to test the individual components of the water balance for a basin, ET estimates have been validated with low errors in the Midwest in the USA, the North China Plain, Sri Lanka and many sites across Australia with all studies on the river basin scale having mean absolute errors less than 5% based on water accounting calculations. These error estimates on the river basin scale include a few METRIC studies and a prior model it is based on (SEBAL). Along with the successful use of METRIC in estimating ET in agricultural areas in Idaho and other regions explain the high reliability and accuracy associated with METRIC estimates in a variety of settings.

The patterns identified based on the variation in the effect on ET in the thinned plots in the Sacramento Mountains require further data to quantify in terms of how the extent of thinning treatment and terrain parameters are related to the extent of the effect on ET but the observed patterns highlight METRIC's ability to capture small-scale variations of ET in complex terrain at high precision. Using a BACI approach to quantify the impact on ET helps to minimize errors in the analysis by comparing differences in estimates of ETrF between thinned and control plots rather than absolute values. While individual ETrF or ET estimates may have larger errors and uncertainty, the high precision associated with METRIC and robust procedure should have consistent and similar errors between the same areas for different years. Therefore, estimates of net impact on ET from differences between estimates should minimize the systematic error in ET estimates from METRIC, which is supported by the similar differences in ET found between thinned and controlled plots in the May and July images prior to thinning. The ETrF values from METRIC fall within the range of expected values found in the literature for mixed coniferous forests and the net effect of thinning on ET for the ridge plots is remarkably similar to those

recently found in a comparable thinning study in a semi-arid upland coniferous forest setting. The extent of the effect on ET in the Sacramento Mountains is undoubtedly tied to the amount of treatment as well the soil and terrain characteristics of the area thinned as is seen by the difference in response between ridge and thinned plots. However in all of the plots thinned, net reductions in ET were found with statistical analysis demonstrating the range of mean net effect on ET had a net decrease for all treated plots at the 98% confidence level. Analysis of METRIC derived ET estimates in the Sacramento Mountains watershed before and after treatment provides evidence that thinning reduces ET within this area in the initial season following thinning.

References

Allen, R. G., M. Tasumi, and R. Trezza (2007), Satellite-based energy balance for mapping evapotranspiration with internalized calibration (METRIC) - Model, *J. Irrig. Drainage Eng-ASCE*, *133*(4), 380–394, doi:10.1061/(ASCE)0733-9437(2007)133:4(380).

Allen, R., A. Irmak, R. Trezza, J. M. H. Hendrickx, W. Bastiaanssen, and J. Kjaersgaard (2011), Satellite-based ET estimation in agriculture using SEBAL and METRIC, *Hydrol. Process.*, *25*(26), 4011–4027, doi:10.1002/hyp.8408.

Dore, S., M. Montes-Helu, S. C. Hart, B. A. Hungate, G. W. Koch, J. B. Moon, A. J. Finkral, and T. E. Kolb (2012), Recovery of ponderosa pine ecosystem carbon and water fluxes from thinning and stand-replacing fire, *Global Change Biology*, *18*(10), 3171–3185, doi:10.1111/j.1365-2486.2012.02775.x.

Kalma, J. D., T. R. McVicar, and M. F. McCabe (2008), Estimating Land Surface Evaporation: A Review of Methods Using Remotely Sensed Surface Temperature Data, *Surv. Geophys.*, *29*(4-5), 421–469, doi:10.1007/s10712-008-9037-z.

Karimi, P., and W. G. M. Bastiaanssen (2015), Spatial evapotranspiration, rainfall and land use data in water accounting -- Part 1: Review of the accuracy of the remote sensing data, *Hydrology & Earth System Sciences*, *19*(1), 507–532, doi:10.5194/hess-19-507-2015.

McWhorter, D. B., and D. K. Sunada (1977), *Ground-water Hydrology and Hydraulics*, Water Resources Publication.

Newman, B. D., B. P. Wilcox, S. R. Archer, D. D. Breshears, C. N. Dahm, C. J. Duffy, N. G. McDowell, F. M. Phillips, B. R. Scanlon, and E. R. Vivoni (2006), Ecohydrology of water-limited environments: A scientific vision, *Water Resour. Res.*, *42*(6), W06302, doi:10.1029/2005WR004141.

Pôças, I., T. A. Paço, M. Cunha, J. A. Andrade, J. Silvestre, A. Sousa, F. L. Santos, L. S. Pereira, and R. G. Allen (2014), Satellite-based evapotranspiration of a super-intensive olive orchard: Application of METRIC algorithms, *Biosystems Engineering*, *128*, 69–81, doi:10.1016/j.biosystemseng.2014.06.019.

Smith, E. P. (2014), BACI Design, in *Wiley StatsRef: Statistics Reference Online*, John Wiley & Sons, Ltd.

Verstraeten, W. W., B. Muys, J. Feyen, F. Veroustraete, M. Minnaert, L. Meiresonne, and A. De Schrijver (2005), Comparative analysis of the actual evapotranspiration of Flemish forest and cropland, using the soil water balance model WAVE, *Hydrol. Earth Syst. Sci.*, *9*(3), 225–241, doi:10.5194/hess-9-225-2005.